

Modal analysis of railway current collectors using Autodesk Inventor

Andrzej Wilk^{*1}, Sławomir Judek¹, Krzysztof Karwowski¹, Mirosław Mizan¹, and Paweł Kaczmarek¹

¹Gdansk University of Technology, Faculty of Electrical and Control Engineering, ul. Gabriela Narutowicza 11/12, 80-233, Gdańsk, Poland

Abstract. The paper presents the results of modal analysis of railway current collector type 160EC. In the first place, the analysis was carried out analytically for a simplified two lumped mass pantograph model. Then numerical analysis was conducted in the Autodesk Inventor (AI) on the prepared multibody model using the AI modal analysis algorithm, which is based on the finite element method (FEM). Model elements which are most relevant for attaining a correct representation of vibration properties when using AI modal analysis were indicated. The influence of selected parameters of modal analysis algorithm on results accuracy was investigated, e.g. the FEM mesh density. The natural frequencies and shapes of the first few vibration modes are shown. The results indicate that the frequencies of natural vibrations of the moving pantograph components are within the range of up to tens of hertz. The possible use of results of pantograph modal analysis at the design stage and in the operation phase was also discussed.

1 Introduction

The development of high-speed railways requires that modern current collectors, apart from the correct static characteristics, must be characterized by special dynamic properties to provide uninterrupted contact between the contact wire and the contact strips of the slipper [1-4]. The pantographs' dynamic properties depend on the accepted design solutions, e.g. detailed construction of drive system, but also on the adjustment of parameters e.g. inertia of components, friction parameters, aerodynamic resistance, etc. [5-8]. It is expedient to analyse and pre-evaluate the construction of the pantograph and the proper selection of its parameters already at the design stage.

Modern methods of current collectors designing use software packages of CAD, CAM and CAE (Computer Aided Design / Manufacturing / Engineering) type. Recently, software manufacturers strive to integrate the CAD/CAM/CAE processes into one complex program, enabling the implementation of optimization procedures. Among a number of software packages that integrate these processes, one of the more popular is Autodesk Inventor (AI) [9]. The AI environment provides convenient geometric designing of models with respect to manufacturing technology and the possibility of parameterization of executive documentation, which is an advantage in the case of a product intended for manufacturing in many variants. AI software allows to providing static and dynamic structural strength analysis of a device, as well as its frequency- and modal analysis [10]. The AI environment allows efficient and comprehensive modelling and analysis of even very complex three-dimensional (3D) structures.

Modal analysis is used both in theoretical and experimental studies to analyse dynamic properties of technical objects - especially mechanical ones. The theoretical modal analysis uses a physical model of the object including its mass, stiffness and damping properties, taking into account their spatial distributions, which leads to the determination of mass, stiffness and damping matrices. Elements of these matrices are the coefficients of a system of normal differential equations of motion. The superposition principle of a linear dynamic system enables the transformation of these equations into a typical eigenvalue problem. Its solution called a modal data of the system is obtained in the form of a set of natural frequencies of simple harmonic motions, mode shapes and damping factors, which allow to predict the behaviour of an object in case of any disturbance of its equilibrium.

The results of modal analysis are used for: structural modifications, diagnostics of structure condition, synthesis of control device in active systems for vibration suppression, and verification and validation of numerical models such as finite element models [11-14]. Currently, many commercial simulation software suits based on the finite element method (FEM) allow the creation of discrete models of almost any linear dynamic structure, which remarkably enlarges the capacity and range of theoretical modal analysis.

2 Modal analysis of pantograph two degrees of freedom

The 3D model of a pantograph in interaction with overhead contact line, which was created in Autodesk Inventor, is presented in Fig. 1a. Alternatively, Fig. 1b

* Corresponding author: andrzej.wilk@pg.edu.pl

shows the simple linear, viscous-damped, lumped parameter model of the current collector, as a more commonly used version in pantograph dynamic simulations [15, 16, 10]. It is a relatively simple conventional lumped mass model consisting of two equivalent masses, connected by springs and damping elements, representing the main components of pantograph, such as panhead, and arms. The model with one degree of freedom (DOF) is not considered here because the response frequency is relatively low. Even more a simple one-mass model with one-DOF, sporadically used to simulate selected phenomena such as waveform of contact force or contact wire uplift, is not considered here because it does not reflect too many significant physical quantities. Also, its response frequency is relatively low.

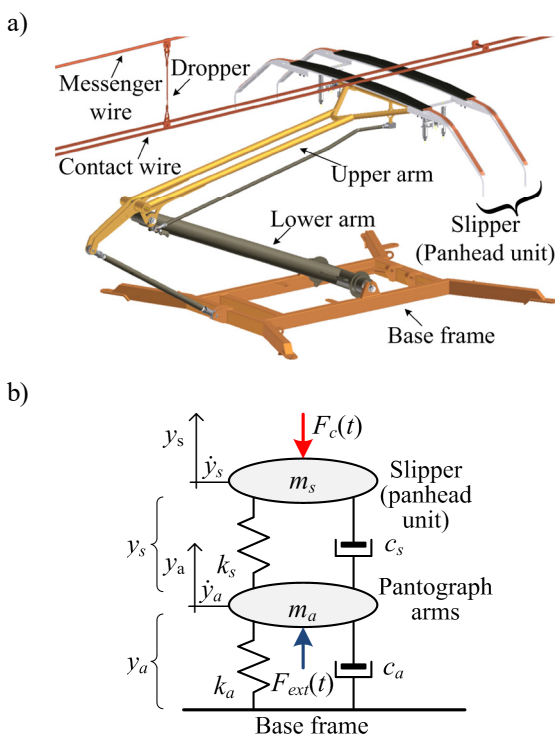


Fig. 1. Current collector in interaction with overhead contact line: a) 3D CAD sketch excluding drive system; b) equivalent lumped two-mass model.

The pantograph model (Fig. 1b) is a two-DOF system which can be described, omitting gravity forces, by an equation of motion in matrix notation as [5, 13]:

$$\begin{bmatrix} m_a & 0 \\ 0 & m_s \end{bmatrix} \begin{bmatrix} \ddot{y}_a \\ \ddot{y}_s \end{bmatrix} + \begin{bmatrix} c_a + c_s & -c_s \\ -c_s & c_s \end{bmatrix} \begin{bmatrix} \dot{y}_a \\ \dot{y}_s \end{bmatrix} + \begin{bmatrix} k_a + k_s & -k_s \\ -k_s & k_s \end{bmatrix} \begin{bmatrix} y_a \\ y_s \end{bmatrix} = \begin{bmatrix} F_{ext} \\ -F_c \end{bmatrix} \quad (1)$$

where: m_a , c_a , k_a , m_s , c_s , k_s represent the equivalent masses, dumping coefficients and stiffness of element of the model for pantograph arm and slipper respectively, F_{ext} is the static lift force, F_c is the contact force.

Since the static lift force F_{ext} is constant and does not affect the vibration characteristic of the pantograph, F_{ext} can be neglected. The change of the contact force F_c and

interaction of overhead contact line are also omitted. The modal analysis was performed for the pantograph only.

Passing to matrix notation the equation (1) becomes:

$$\mathbf{M}\ddot{\mathbf{y}} + \mathbf{C}\dot{\mathbf{y}} + \mathbf{K}\mathbf{y} = \mathbf{F} \quad (2)$$

where: \mathbf{M} , \mathbf{C} and \mathbf{K} are the mass, damping and stiffness matrices respectively; \mathbf{y} , $\dot{\mathbf{y}}$ and $\ddot{\mathbf{y}}$ are the corresponding displacement, velocity and acceleration and \mathbf{F} represents forces applied to the pantograph.

In case of an undamped and unforced system the matrices and vectors from (2) become:

$$\mathbf{M} = \begin{bmatrix} m_a & 0 \\ 0 & m_s \end{bmatrix}, \quad \mathbf{C} = \begin{bmatrix} 0 & 0 \\ 0 & 0 \end{bmatrix}, \quad \mathbf{K} = \begin{bmatrix} k_a + k_s & -k_s \\ -k_s & k_s \end{bmatrix},$$

$$\mathbf{F} = \begin{bmatrix} 0 \\ 0 \end{bmatrix}, \quad \mathbf{y} = \begin{bmatrix} y_a \\ y_s \end{bmatrix}. \quad (3)$$

As a result, the notation of equation (2) reduces to:

$$\mathbf{M}\ddot{\mathbf{y}} + \mathbf{K}\mathbf{y} = \mathbf{0} \quad (4)$$

Assuming a solution in the form of: $\mathbf{y}(t) = \mathbf{Y}e^{i\omega t}$, which leads to: $\ddot{\mathbf{y}}(t) = -\omega^2 \mathbf{Y}e^{i\omega t}$, it can be expressed as:

$$[\mathbf{K} - \omega^2 \mathbf{M}]\mathbf{Y} = \mathbf{D}(\omega)\mathbf{Y} = \mathbf{0} \quad (5)$$

where: \mathbf{Y} is a nonzero two-element vector that represents the amplitudes of the motions of the point masses, and

$\mathbf{D}(\omega) = [\mathbf{K} - \omega^2 \mathbf{M}]$ is called the dynamic matrix.

Equation (5) states the free vibrations eigenproblem for an undamped two-DOF system. For nontrivial solutions $\mathbf{Y} \neq \mathbf{0}$ the determinant of the dynamic matrix must become zero:

$$\det \mathbf{D}(\omega) = \det[\mathbf{K} - \omega^2 \mathbf{M}] = 0 \quad (6)$$

This forms the characteristic equation for free undamped vibrations. For a two-DOF system, the left side of (6) has a form of quadratic polynomial of variable ω^2 , which yield two roots: ω_1^2 and ω_2^2 .

Assuming a set of typical values of pantograph equivalent masses $m_a = 37.12$ kg, $m_s = 19.87$ kg and stiffness $k_a = 50$ N/m, $k_s = 16000$ N/m, the equation (6) takes a notation of:

$$\det \begin{bmatrix} 16050 - 37.12\omega^2 & -16000 \\ -16000 & 16000 - 19.87\omega^2 \end{bmatrix} =$$

$$= 737.6\omega^4 - 912833.5\omega^2 + 800000 = 0 \quad (7)$$

The roots of equation (7) are real and nonnegative numbers:

$$\omega_1^2 = 0.877(\text{rad/s})^2 \quad \text{and} \quad \omega_2^2 = 1236.74(\text{rad/s})^2 \quad (8)$$

called as the undamped natural circular frequencies.

Vectors $\mathbf{Y}_1(\omega_1)$ and $\mathbf{Y}_2(\omega_2)$ are mathematically called as eigenvectors:

$$\mathbf{Y}_1 = \begin{bmatrix} 1 \\ 1.0011 \end{bmatrix} \text{ and } \mathbf{Y}_2 = \begin{bmatrix} 1 \\ -1.8661 \end{bmatrix} \quad (9)$$

Note that in the first mode (ω_1) the masses oscillate in phase while in the second one (ω_2) they move opposite to each other. The visualization of an eigenvector as a motion pattern is called a mode shape of the system.

Normalization criteria are often used in the analysis i.e. the highest absolute value of \mathbf{Y}_i is searched, and then \mathbf{Y}_i is divided by it. Normalized eigenvector is called Φ , for assumed parameters of two-DOF pantograph model it is as follows:

$$\Phi_1 = \begin{bmatrix} 0.9989 \\ 1.0 \end{bmatrix} \text{ and } \Phi_2 = \begin{bmatrix} 0.5359 \\ -1.0 \end{bmatrix} \quad (10)$$

After orthogonalization and orthonormalization it is possible to write modal equation of motion for generalized coordinates [13] as:

$$\mathbf{M}_g \ddot{\boldsymbol{\eta}} + \mathbf{K}_g \boldsymbol{\eta} = \mathbf{0} \text{ or short } \ddot{\boldsymbol{\eta}} + \mathbf{K}_g \boldsymbol{\eta} = \mathbf{0} \quad (11)$$

where: $\mathbf{M}_g = \Phi^T \mathbf{M} \Phi = \mathbf{I}$ is generalised mass matrix, that reduces to the identity matrix \mathbf{I} hence in short notation it may be omitted, $\mathbf{K}_g = \Phi^T \mathbf{K} \Phi = \text{diag}[\omega_i^2]$ is generalised stiffness matrix, and $\boldsymbol{\eta}$ is generalised coordinates vector.

Because the matrices \mathbf{M}_g and \mathbf{K}_g are diagonal, equation (11) uncouples into two homogeneous, ordinary second order differential equations already in canonical form. Once solutions η_a and η_s are available, they can be combined via the superposition procedure to get the physical response:

$$\mathbf{y}(t) = \Phi \boldsymbol{\eta}(t) \quad (12)$$

To solve this equation, its initial conditions in modal coordinates are needed. For analysed example of two-DOF pantograph model the solution in generalised and physical coordinates for exemplary initial conditions

$\mathbf{y}_0 = \begin{bmatrix} 0 \\ 0 \end{bmatrix}$, $\mathbf{v}_0 = \begin{bmatrix} 1 \\ 0 \end{bmatrix}$ are respectively:

$$\boldsymbol{\eta} = \begin{bmatrix} 5.2486 \sin(0.936t) \\ 0.1024 \sin(35.167t) \end{bmatrix} \quad (13)$$

$$\mathbf{y} = \Phi \boldsymbol{\eta} = \begin{bmatrix} 0.6950 \sin(0.936t) + 0.0099 \sin(35.167t) \\ 0.6957 \sin(0.936t) - 0.0185 \sin(35.167t) \end{bmatrix} \quad (14)$$

$$\dot{\mathbf{y}} = \mathbf{v} = \begin{bmatrix} 0.6508 \cos(0.936t) + 0.3492 \cos(35.167t) \\ 0.6516 \cos(0.936t) - 0.6516 \cos(35.167t) \end{bmatrix} \quad (15)$$

Fig. 2 shows waveforms of displacements \mathbf{y} and velocities \mathbf{v} for the two DOF model of current collector (see: Fig. 1b).

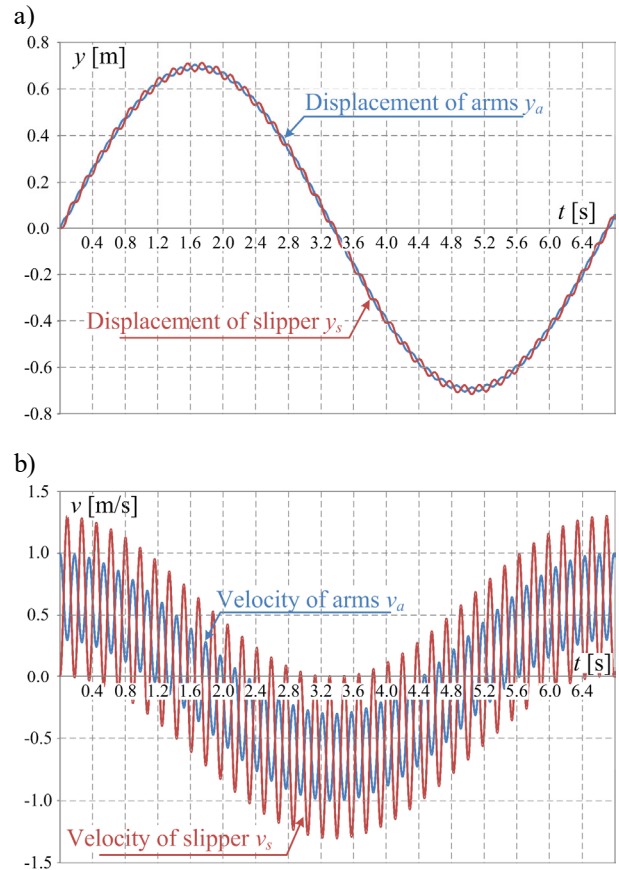


Fig. 2. Response waveforms for analytical modal analysis for lumped mass model of pantograph for arms and slipper respectively: a) displacements y_a, y_s ; b) velocities v_a, v_s .

In the case of the damped system, using (1) and (2), the equation (11) will take the following form:

$$\ddot{\boldsymbol{\eta}}(t) + \mathbf{C}_g \dot{\boldsymbol{\eta}}(t) + \text{diag}(\omega_i^2) \boldsymbol{\eta}(t) = \mathbf{f}(t) \quad (16)$$

where: \mathbf{M}_g is reduced to the identity matrix \mathbf{I} therefore it was omitted in the notation above, \mathbf{K}_g becomes a diagonal matrix with squared frequencies stacked along its diagonal, $\mathbf{f}(t)$ is called a modal forces vector, the modal matrix \mathbf{C}_g generally will not be a diagonal matrix. For such case, it is not possible to decoupling of modal equation of motion.

The above example shows that modal analysis for a highly simplified current collector model can be carried out even analytically at relatively low time, especially in the case of omitting the damping phenomena, but it provides little information – in practice it is only possible to determine the basic vibration frequencies of the main components of the pantograph in this way.

3 Computer modelling of current collectors in Autodesk Inventor

In order to perform a comprehensive simulation analysis of the pantograph using AI, it is necessary to develop its basic physical model. The main operations at model creating and at modal analysis of the current collector in this environment are presented in Fig. 3.

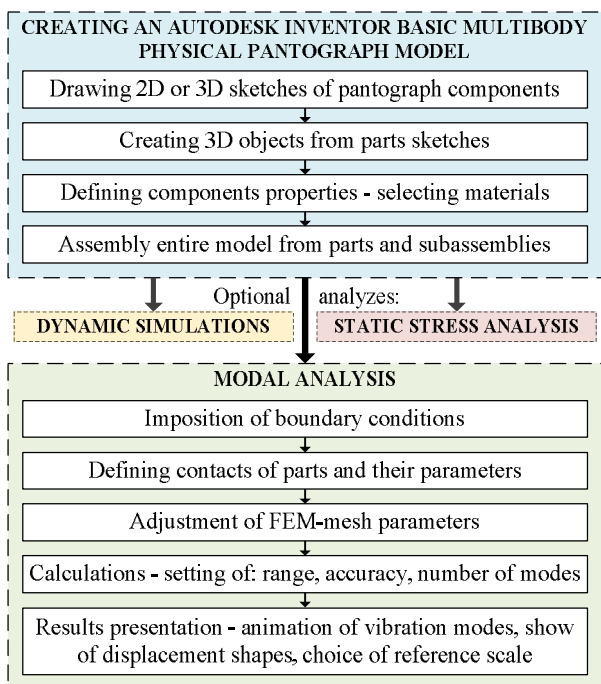


Fig. 3. Flowchart of pantograph modal analysis using Autodesk Inventor.

The process of modelling is typical in AI, although it should be noted, that some stages may be difficult because e.g. such materials as carbon for contact strips are not included in program library. For proper reflection of dynamic properties at modal analysis it is necessary to determine relevant parameters of those materials such as density, elasticity, Young's modulus etc. The correct determination of the types of mechanical contacts between pantograph parts together with the adoption of adequate values of contact parameters especially for mutually moving parts is of particular importance. In modal analysis AI allows only to define two types of contacts: bonded and spring, for the latter it is possible to independently set the normal and tangential stiffness. This process requires a lot of engineering experience, as these values affect the results of the collector eigenvibrations frequencies. Another important task is to set the parameters of FEM-mesh, especially in places of spring contacts, because its automatic generation can cause significant inaccuracy of analysis results. The program allows selective mesh densification in areas indicated by the user.

Figure 4a shows the prepared basic physical model of the pantograph with its main components marked. Figure 4b presents an enlarged part of the suspension system of the pantograph head. For obtaining representative results in modal analysis, this subassembly must be modelled with relatively high precision because it has a significant influence on the dynamic properties of the current collector. Particularly essential is the precise elaboration of the suspension springs model, wherein apart from the proper indication of material and dimensions, it is important to correctly place them in the nests and also appropriately set the density of the FEM-mesh, what is shown on Fig. 4c.

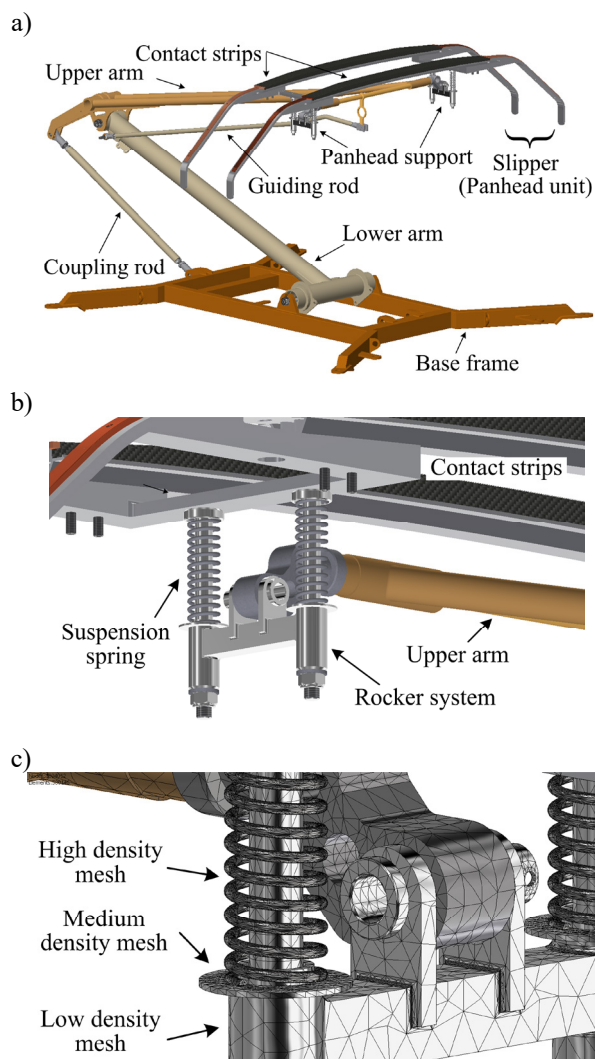


Fig. 4. Autodesk Inventor model (excluding drive system) of 160EC railway current collector: a) entire pantograph with marked main parts; b) slipper suspension unit; c) enlarged fragment of suspension unit with superimposed FEM-mesh.

4 Finite element modal analysis results

Based on the created AI model of the current collector, the modal analysis was performed. In the first stage, the study concerned only the slipper unit together with its suspension system, which was separated from the rest of the device. Among other, the aim was to determine the right FEM-mesh density distribution based on the comparison of the obtained frequency of slipper's basic vibration mode with the results derived from the simplified two-mass model analysis (see Section 2) and from the laboratory experiment. Fig. 5 shows the displacement shapes and frequencies of the first three vibration modes of the slipper unit. The vibrations represented by modes 1 and 2 are of major importance in the interaction between the pantograph and the overhead contact line – note that their frequencies are very close. It can be stated that the oscillation of the upper mass in the equivalent lumped two-mass model is mainly a superposition of these two modes of vibration, and therefore its frequency should be within the interval

determined by two obtained values. Achieved results fulfill this condition.

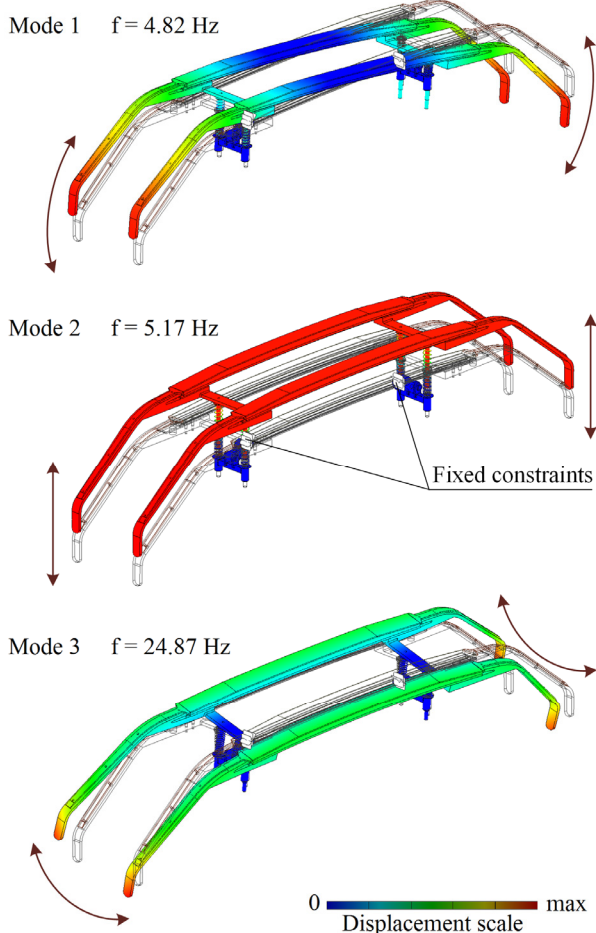


Fig. 5. Displacement shapes and corresponding frequencies of the first three vibration modes of the slipper unit obtained by AI modal analysis.

If the slipper is treated as a lumped mass, then the natural frequency can be calculated as:

$$f = \frac{1}{2\pi} \sqrt{\frac{k}{m}} = \frac{1}{2\pi} \sqrt{\frac{16188}{16.06}} = 5.05 \text{ Hz} \quad (17)$$

where k is equivalent stiffness of suspension springs, m is the sum of the masses of the components of the slipper. Obtained values correspond to mode 2 presented in Fig. 5.

Subsequently, an analysis was performed for the entire pantograph, but without the drive system, for the selected uplift height within the normal operating range. The results for vibration modes with frequencies up to about 25 Hz are shown on Fig. 6. It should be noted that in modal analysis of the AI the graphically presented displacements are relative, i.e. they are scaled in relation to their highest value in a given vibration mode. This way they do not reflect the real absolute magnitude of deviations. On the Fig. 5 and Fig. 6, the fixed constraints i.e. the locations of the rigid mounting of the analyzed device are indicated, which constitute the boundary conditions for modal analysis.

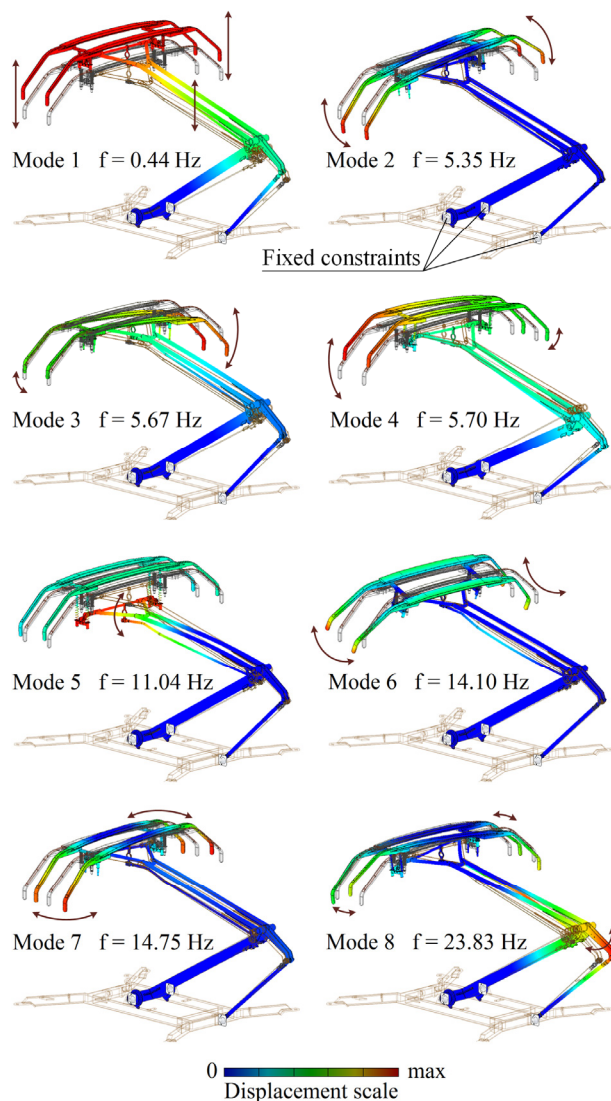


Fig. 6. Displacement shapes and corresponding frequencies of the pantograph eigenvibration modes with frequencies up to 25 Hz obtained by AI modal analysis.

It can be seen that the frequency of the collector first vibration mode is consistent in range magnitude with the lower frequency obtained from the analytical calculations of the two-mass model (see Section 2). It should be emphasized, however, that the created AI pantograph model does not cover its drive system yet – the work in this field continues, hence the difference between both values is noticeable. On the other hand, the frequencies of the main vibration modes of the slipper unit – modes No 2, 3, 4 – have not changed significantly with respect to results given above for the unit separated from pantograph arms.

Looking at the pantograph vibration modes obtained by modal analysis, some of them associated with spring connection of the components are of practical importance in studying the dynamic interaction between the current collector and the overhead contact line, but the other result from the inevitable existence of clearance in articulated joints or from the limited rigidity of the long components e.g. lower and upper arm or slipper contact strips. The latter modes may be more interesting rather at the design stage than in the operational phase,

while the first group gives information that can be used at the exploitation check of the collector's technical condition.

5 Conclusions

Performed modal analysis indicates that the frequencies of the excited natural vibrations of the moving pantograph components are within the range of up to tens of hertz. Higher frequencies generally involve harmonic distortions of components or vibrations caused by a slight clearance in moving links. Such marginal phenomena have a negligible effect in normal operation of the pantograph. The comparison of the results obtained for main vibration modes of the full-bodied AI-model with the results obtained for the simplified model, e.g. with two degrees of freedom, allows for the adjustment or verification of equivalent parameters of the latter. Simple lumped parameters models with a small number of degrees of freedom are often used in simulation procedures for assessing the quality of dynamic co-operation between overhead lines and current collectors – as required by certification procedures for newly developed or renovated overhead contact lines. The use of a precise 3D-multibody FEM-model in this case is not justified and would lead to significant complications and increased workload.

The results presented in this article are of preliminary nature - currently the work is focused on completing the AI pantograph model including its propulsion system. Future study will concern the impact of changes in the most important parameters of the current collectors, related to the wear and deterioration of individual components, and will also focus on the frequencies and mode shapes of the eigenvibrations of the device. This may be a premise to use the results of modal analysis in the technical diagnostics of pantographs.

References

1. J. Jiang, Z. Liu, and X. Lu, Optimization of the pantograph parameters based on matching performance between pantograph parameters and dropper interval, *Proceedings of the 35th Chinese Control Conference*, 9742–9747 (2016)
2. J.-P. Massat, C. Laurent, J.-P. Bianchi, and E. Balmès, *Pantograph catenary dynamic optimisation based on advanced multibody and finite element co-simulation tools*, *Vehicle System Dynamics*, **52**, 338–354 (2014)
3. T.X. Wu, and M.J. Brennan, *Active vibration control of a railway pantograph*, *Proc. Inst. Mech. Eng. Part F: Journal of Rail Rapid Transit*, **211**, 117–130 (1997)
4. T.X. Wu, and M.J. Brennan, *Basic Analytical Study of Pantograph-catenary System Dynamics*, *Vehicle System Dynamics*, **30**, 443–456 (1998)
5. J. Ambrósio, F. Rauter, J. Pombo, and M.S. Pereira, *A Flexible Multibody Pantograph Model for the Analysis of the Catenary–Pantograph Contact*, in: K. Arczewski, W. Blajer, J. Fraczek, M. Wojtyra, (Eds.), *Multibody Dynamics: Computational Methods and Applications*. Springer Netherlands, Dordrecht, 1–27 (2011)
6. J.P. Bianchi, E. Balmès, G.V. des Roches, and A. Bobillot, Using modal damping for full model transient analysis. Application to pantograph/catenary vibration, *Proc. of the Int. Conf. on Adv. Acoustics and Vibration Eng. ISMA 2010, Leuven Belgium*, 1167-1180 (2010)
7. C. Zhao, N. Zhou, H. Zou, R. Li, R., and W. Zhang, Comparison of dynamic characteristics of different pantograph models, *Proceedings of the 35th Chinese Control Conference*, 10216–10221 (2016)
8. N. Zhou, W. Zhang, and R. Li, *Dynamic performance of a pantograph-catenary system with the consideration of the appearance characteristics of contact surfaces*, *Journal of Zhejiang University-SCIENCE A*, **12**, 913–920 (2011)
9. AUTODESK Inventor, <http://www.autodesk.pl/products/inventor/overview>
10. A. Wilk, K. Karwowski, S. Judek, and M. Mizan, A new approach to determination of the two-mass model parameters of railway current collector, *12th Int. Conf. Modern Electrified Transport MET'2015, Trogir, Croatia*, 164-170 (2015).
11. S. Judek, and L. Jarzebowicz, *Wavelet Transform-Based Approach to Defect Identification in Railway Carbon Contact Strips*, *Elektronika I Ir Elektrotehnika*, **21** (6), 29-33 (2015)
12. Karwowski, K., Mizan, M., Karkosiński, D., *Monitoring of current collectors on the railway line*, *Transport*, **33**, 177–185 (2018)
13. P. Lengvarský, and J. Bocko, *Theoretical Basis of Modal Analysis*, *Am. J. Mech. Eng.*, **1** (7), 173–179 (2013)
14. G. Santamato, M. Solazzi, and A. Frisoli, A Detection Method of Faults in Railway Pantographs Based on Dynamic Phase Plots, *World Acad. Sci. Eng. Technol. Int. J. of Mech. and Mechatr. Eng.*, **10** (8), 1474-1485 (2016)
15. Commission Regulation (EU) No 1301/2014 of 18 November 2014 on the technical specifications for interoperability relating to the ‘energy’ subsystem of the rail system in the Union (2104)
16. EN 50318, *Railway applications. Current collection systems. Validation of simulation of the dynamic interaction between pantograph and overhead contact line* (2003)